RESEARCH ARTICLE

WILEY

Abnormal amygdala functional connectivity and deep learning classification in multifrequency bands in autism spectrum disorder: A multisite functional magnetic resonance imaging study

Huibin Ma[1] | Yikang Cao[1] | Mengting Li[2,3] | Linlin Zhan[4] | Zhou Xie[1] |
Lina Huang[5] | Yanyan Gao[2,3] | Xize Jia[5] (ID)

[1]School of Information and Electronics Technology, Jiamusi University, Jiamusi, China

[2]College of Teacher Education, Zhejiang Normal University, Jinhua, China

[3]Key Laboratory of Intelligent Education Technology and Application, Zhejiang Normal University, Jinhua, China

[4]Faculty of Western Languages, Heilongjiang University, Harbin, China

[5]Department of Radiology, Changshu No. 2 People's Hospital, The Affiliated Changshu Hospital of Xuzhou Medical University, Changshu, China

Correspondence
Xize Jia, Department of Radiology, Changshu No. 2 People's Hospital, The Affiliated Changshu Hospital of Xuzhou Medical University, Changshu, Jiangsu, China
Email: jiaxize@foxmail.com

Yanyan Gao, College of Teacher Education, Zhejiang Normal University; Key Laboratory of Intelligent Education Technology and Application of Zhejiang Province, Zhejiang Normal University, Jinhua 321004, China
Email: gaoyanyan1999@163.com

Abstract

Previous studies have explored resting-state functional connectivity (rs-FC) of the amygdala in patients with autism spectrum disorder (ASD). However, it remains unclear whether there are frequency-specific FC alterations of the amygdala in ASD and whether FC in specific frequency bands can be used to distinguish patients with ASD from typical controls (TCs). Data from 306 patients with ASD and 314 age-matched and sex-matched TCs were collected from 28 sites in the Autism Brain Imaging Data Exchange database. The bilateral amygdala, defined as the seed regions, was used to perform seed-based FC analyses in the conventional, slow-5, and slow-4 frequency bands at each site. Image-based meta-analyses were used to obtain consistent brain regions across 28 sites in the three frequency bands. By combining generative adversarial networks and deep neural networks, a deep learning approach was applied to distinguish patients with ASD from TCs. The meta-analysis results showed frequency band specificity of FC in ASD, which was reflected in the slow-5 frequency band instead of the conventional and slow-4 frequency bands. The deep learning results showed that, compared with the conventional and slow-4 frequency bands, the slow-5 frequency band exhibited a higher accuracy of 74.73%, precision of 74.58%, recall of 75.05%, and area under the curve of 0.811 to distinguish patients with ASD from TCs. These findings may help us to understand the pathological mechanisms of ASD and provide preliminary guidance for the clinical diagnosis of ASD.

KEYWORDS
autism spectrum disorder, deep learning, deep neural network, frequency-specific, functional connectivity, generative adversarial networks, image-based meta-analysis

---

Huibin Ma and Yikang Cao contributed equally to this work.

1 | INTRODUCTION

Autism spectrum disorder (ASD) is a neurodevelopmental disorder characterized by impaired social symptoms that often hinder social interaction and communication, as well as remarkable repetitive behaviors (Geschwind & Levitt, 2007; Lord et al., 2018). With an increasing prevalence, serious impairment of ASD has imposed a major burden on health and finance worldwide (Chiarotti & Venerosi, 2020; Fombonne, 2018). However, the neural mechanisms underlying these dysfunctional social symptoms remain poorly understood. Recent evidence has indicated that the deviant social brain network may contribute to social deficiency in ASD (Misra, 2014; Sato et al., 2012; Sato et al., 2017; Sato & Uono, 2019), which affects the ability of patients with ASD to process social information, including facial expression recognition (Lozier et al., 2014; Sato et al., 2012) and social attention processing (Wang, Chen, et al., 2020). The amygdala is a well-known brain region that plays a major role in the social brain network, and its importance in the social brain is widely acknowledged (Li et al., 2021; Skuse et al., 2003). Considering the significance of the amygdala in the social brain, a deeper understanding of the abnormalities in the amygdala might be valuable and constructive to understand the pathological mechanisms of impaired social symptoms in ASD.

Resting-state functional magnetic resonance imaging (rs-fMRI) is a noninvasive neuroimaging tool that has shown great potential to explore the pathological mechanisms of ASD (Huang et al., 2020; Wee et al., 2016; Zhao, Huang, et al., 2020). As one of the most common analytic methods of rs-fMRI, functional connectivity (FC) reflects the interaction of two distinct brain regions (Biswal et al., 2015; Fox & Raichle, 2007) and has presented enormous advantages in revealing disrupted brain connectivity in ASD (Wang et al., 2021; Yao et al., 2021; Zhao et al., 2021). Using the FC approach, researchers have found that altered FC of the amygdala is related to social impairment in patients with ASD. For example, Odriozola et al. (2019) found that altered FC between the amygdala and frontal cortex leads to core socio-emotional impairments in patients with ASD. Shou et al. (2017) have shown that patients with ASD showed a lower FC between the amygdala and supramarginal gyrus (SMG), and the altered FC values were associated with the severity of social symptoms in ASD. These findings support the amygdala theory of autism, indicating that abnormalities in the amygdala are associated with the underlying mechanisms of social impairment in ASD (Baron-Cohen, 2000).

However, previous amygdala-based FC studies of ASD mainly focused on the results of the conventional frequency band of 0.01–0.08 Hz rather than those of the subfrequency bands. Researchers have demonstrated that low-frequency oscillations, especially slow-5 (0.01–0.027 Hz) and slow-4 (0.027–0.073 Hz) subfrequency bands, reflect brain activity from the perspective of gray matter (Zuo et al., 2010). Neural oscillations in distinct frequency bands exhibit different properties and physiological functions (Buzsaki & Draguhn, 2004; Penttonen & Buzsáki, 2003). By examining neural oscillations in the slow-4 and slow-5 frequency bands, alterations in frequency-dependent neural activity have been found to be associated with the pathological mechanisms of some neural diseases, such as acute basal ganglia ischemic stroke (Li, Cheng, et al., 2022), depression (Wang, Kong, et al., 2016), mild cognitive impairment (Wang, Li, et al., 2016), and Alzheimer's disease (AD; Yang, Yan, et al., 2020). These findings indicate that exploring abnormal neural activity in subfrequency bands may provide valuable information on the pathological mechanisms of ASD. Therefore, combining the important role that the amygdala plays in the social dysfunction of ASD, this study aimed to investigate the abnormal FC of the amygdala in the conventional (0.01–0.08 Hz), slow-5 (0.01–0.027 Hz), and slow-4 (0.027–0.073 Hz) frequency bands to reveal the pathological mechanism of ASD.

Moreover, although a large number of rs-fMRI studies have been conducted to reveal abnormal connections between different brain regions in ASD (Di Martino et al., 2017; Duan et al., 2017; Guo et al., 2016; Minshew & Keller, 2010; Tomasi & Volkow, 2019), the results are controversial and inconsistent. As a solution, a meta-analysis could effectively pool the findings of multiple independent rs-fMRI studies to identify the most common results across studies (Radua et al., 2014; Wang et al., 2021). Compared with coordinate-based meta-analysis, image-based meta-analysis (IBMA), which draws on all statistical information of the brain, has a great advantage in revealing significantly consistent differential regions that show great sensitivity and is recommended by researchers (Radua et al., 2012; Salimi-Khorshidi et al., 2009). However, implementing IBMA is challenging because numerous rs-fMRI studies only reported peak statistics and locations rather than the original whole-brain statistical maps. Fortunately, with the establishment and development of neuroimaging data-sharing projects in recent years, IBMA has gradually become possible. As one of the widely used public databases, Autism Brain Imaging Data Exchange (ABIDE; http://fcon_1000.projects.nitrc.org/indi/abide/) has collected rs-fMRI data from multiple brain imaging sites worldwide (Di Martino et al., 2014; Di Martino et al., 2017). Therefore, based on the public dataset ABIDE, an IBMA was performed to obtain reliable results in the conventional, slow-4, and slow-5 frequency bands in this study.

Deep learning methods are a set of methods that allow computational models to be fed with data and can automatically discover the sample features needed for detection or classification (LeCun et al., 2015). They have been widely used in the classification of various diseases, including Parkinson's disease (PD) (Bi et al., 2021), AD (Bi et al., 2022; Ramzan et al., 2020), and ASD (Jiang et al., 2022; Li, Tang, et al., 2022; Shahamiri et al., 2022). Deep neural networks (DNNs), a supervised deep learning model, have been widely used in previous rs-fMRI studies due to their ability to differentiate patients from TCs (Epalle et al., 2021; Supekar et al., 2022; Yang, Schrader, & Zhang, 2020). Furthermore, previous study has found that feature complexity can enhance the effect of classification and robustness of deep learning (Goodfellow et al., 2020). Generative adversarial networks (GANs) can increase feature complexity by generating features (Goodfellow et al., 2020; Park et al., 2021; Yi et al., 2019). Previous deep learning studies that adopted the GANs model have found that the GANs model can improve the classification accuracy of some diseases, including AD (Sinha et al., 2021; Zhou et al., 2021) and major depressive disorder (Zhao, Chen, et al., 2020). Hence, the application

of deep learning using GANs and DNN may provide a new measure to examine whether frequency-specific FC alterations could be used as neuromarkers for ASD.

In this study, based on multisite ABIDE datasets, we used the bilateral amygdala as seed regions to explore whether patients with ASD showed different abnormal FC within different frequency bands (conventional, slow-4, and slow-5 frequency bands). Moreover, we adopted deep learning methods to explore the classification ability of different frequency bands. We hypothesized that the altered FC of the amygdala would be frequency-specific, and that deep learning methods would achieve relatively good classification accuracy, where FC alterations could be used as potential neuromarkers for classification.

2 | MATERIALS AND METHODS

2.1 | Participants and image acquisition

This study obtained data from the ABIDE project (http://fcon_1000.projects.nitrc.org/indi/abide/), which collects functional and structural images of ASD from a number of laboratories worldwide and includes two datasets: ABIDE I (Di Martino et al., 2014) and ABIDE II (Di Martino et al., 2017). In ABIDE I, 1112 participants (539 patients with ASD and 573 TCs) from 17 sites were included. In ABIDE II, 1114 participants (521 patients with ASD and 593 TCs) from 19 sites were included. Written informed consent was obtained from each participant, and all experimental protocols were approved by the local Institutional Review Boards of each institution.

The time points and slice numbers of all rs-fMRI data were checked. Additionally, ABIDE I and ABIDE II were combined based on time points and slice numbers. The exclusion criteria for all participants were the following: (1) inconsistent time points or slice numbers; (2) not right-handed; (3) poor data quality; (4) head motion exceeding 1 mm or $1°$; (5) bad spatial normalization; (6) age or sex mismatch with others at the same site; (7) sites with few participants or lack of TCs.

2.2 | Data preprocessing

All fMRI data preprocessing was performed using the resting-state fMRI Data Analysis Toolkit (RESTplus V1.25, http://restfmri.net/forum/restplus) (Jia et al., 2019) based on statistical parametric mapping (SPM12, https://www.fil.ion.ucl.ac.uk/spm) running on MATLAB 2017b. The preprocessing steps proceeded as follows: (1) discarding the first 10 time points; (2) slice timing correction; (3) head motion correction; (4) spatial normalization to the Montreal Neurological Institute (MNI) space via the deformation field originating from the new segmentation of the structural images and resampled to $3 \times 3 \times 3$ mm^3; (5) spatial smoothing with a 6 mm full width at half maximum (FWHM); (6) linear detrending; (7) nuisance signal regression with the Friston-24 head motion parameters as covariate (Friston

et al., 1996); (8) bandpass filtering in the conventional frequency band (0.01–0.08 Hz), the slow-5 band (0.01–0.027 Hz), and the slow-4 band (0.027–0.073 Hz).

2.3 | FC analysis

After data preprocessing, FC analysis was performed using the fMRI Data Analysis Toolkit RESTplus V1.25 with the bilateral amygdala as seeds (Jia et al., 2019). In accordance with the previous studies (Ambrosi et al., 2017; Guo et al., 2016; Wang, Lyu, et al., 2020), the two seed regions of the bilateral amygdala used in this research were defined based on the anatomical automatic labeling (AAL) template, which was provided by RESTplus V1.25 toolbox (Jia et al., 2019). For the conventional, slow-5, and slow-4 frequency bands, the whole FC maps (r-value) of each seed region were generated by calculating Pearson's correlation coefficient between the average time series of the seed region and every voxel of the whole brain. To improve normality, the r-value was converted into the z-value using Fisher's r to z translation.

2.4 | Statistical analysis

All statistical analyses of demographic information (age and sex) were performed using statistical product and service solutions version (SPSS 26.0, IBM, Armonk, New York). The significance level was set at $p < .05$. For each site, the age and sex of patients with ASD and TCs were compared. The χ^2 test was performed to calculate p-values for sex and the two-sample t-test for age.

To investigate the difference in FC values between the ASD and TC groups, a two-sample t-test was performed at each site using RESTplus V1.25 software (Jia et al., 2019). For each site, a t statistical map without correction was generated.

2.5 | Image-based meta-analysis

In this study, image-based meta-analyses were performed to explore the consistent deviant FC patterns of ASD across all sites in the conventional, slow-5, and slow-4 frequency bands via anisotropic effect-size signed differential mapping (AES-SDM) (Radua et al., 2014). First, each voxel was assigned a measure of effect size, known as the standardized mean difference. Second, an uncorrected t map was used to derive the effect size map and its variance map for each site. Third, weighted by the sample size of each site, the effect size map and variance maps of all sites were integrated using the random-effects model. Finally, the mean effect size map created using the results of the third step was converted into a z-map. Furthermore, an uncorrected $p < .0001$ (Wang et al., 2022) was chosen to optimize false-positive results in this study. Other parameters (full anisotropy = 1.0, FWHM = 20 mm, Monte Carlo randomization = 20, $Z > 1$, and cluster size >10 voxels) were also used in this study.

2.6 | Classification using a deep learning approach

2.6.1 | FC-matrix construction

By conducting bilateral amygdala-based whole-brain FC analyses, two whole-brain FC maps (r-values) of each participant were generated in each frequency band. The original r-value of the FC was then converted to the normally distributed z-value using Fisher's r to z transformation. Based on the whole-brain FC maps (z-value) of each participant, we extracted the averaged z-value of all voxels in the region of interest (ROI) identified from the AAL atlas, which comprises 90 ROIs (Tzourio-Mazoyer et al., 2002). Since there were both left and right amygdala-based whole-brain z-maps, a 2×90 FC matrix was constructed for each participant in the conventional, slow-4, and slow-5 frequency bands.

2.6.2 | Feature generation using GANs

To enhance the classification ability of the DNN, the GANs model was used to generate features based on the original FC matrices of this study (Goodfellow et al., 2020). The GANs model contains one generative network and one discriminated network. The generative network has four fully connected layers that employ a hyperbolic tangent (tanh) function as the activation function. The discriminant network also consisted of four fully connected layers: the first three layers used tanh activation functions, and the fourth layer used the sigmoid activation function. To improve the generalization of the model, we added a dropout layer after each fully connected layer to reduce overfitting; the dropout size was set to 0.3. In the training process, Adam optimizer was applied to minimize the loss of the GANs model. The learning rates for both the generative and discriminate networks were set at 0.0002. The batch size was set at 32, and the maximum number of iterations was set at 8000.

Based on the original 2×90 FC matrices of 306 patients with ASD and 314 TCs, the 2×90 FC matrices of 150 patients with ASD and 150 TCs were generated using GANs. Finally, 2×90 FC matrices of 456 patients with ASD and 464 TCs were constructed and used as the input for subsequent DNN classification.

2.6.3 | Classification using DNN

In this study, a DNN algorithm was implemented to evaluate whether amygdala-based whole-brain FC values in different frequency bands have different diagnostic abilities for ASD (Shahamiri et al., 2022). The 2×90 FC matrices of 456 patients with ASD and 464 TCs were defined as input features for deep learning. Moreover, to present the improvement of the GANs in the classification ability of deep learning, deep learning without applying the GANs was performed based on the 2×90 FC matrices of 306 patients with ASD and 314 TCs.

In the training process, a binary classification task was involved; therefore, we applied binary cross-entropy to examine the effect of the loss function. All training processes were performed under the deep learning framework TensorFlow with the Adadelta optimization algorithm. To reduce overfitting, the L1-norm and L2-norm regulation parameters were applied. In the training process, the learning rate was set to 0.0025, the batch size was set to 256, and the maximum number of iterations was set to 7000. The neural network consisted of five fully connected layers, the first four layers using tanh activation functions, and the last layer using sigmoid activation functions. To further reduce overfit susceptibility, we used three dropout layers after applying three medium fully connected layers, the value of which was set to 0.3.

3 | RESULTS

3.1 | Demographic and clinical information

In this study, 28 patients with ASD and 30 TCs were excluded due to inconsistent time points or slice numbers. After merging the sites, 2168 participants (1032 patients with ASD and 1136 TCs) from 34 sites were collected. Furthermore, 131 patients with ASD and 105 with TCs were ruled out because they were not right-handed. Due to impaired functional or structural imaging, 17 patients with ASD and 7 TCs were excluded. Due to excessive head movement (>1 mm or 1°), 460 patients with ASD and 481 TCs were excluded. Bad spatial normalization led to the exclusion of 40 patients with ASD and 49 TCs. In addition, 20 patients with ASD and 167 TCs were excluded due to a mismatch in age or sex. Moreover, four sites that included 58 patients with ASD and 13 TCs were excluded because they had few participants or lacked TCs. Based on the above exclusion criteria, this study collected data from 28 sites, including 306 patients with ASD and 314 TCs. Detailed information on the exclusion criteria is described in Table S1.

For all sites included in this study, there were no significant differences in age or sex between the ASD and TCs groups ($p > .05$). Table 1 presents the statistical results.

3.2 | The meta-analysis results in multifrequency band

3.2.1 | Altered FC results of the left amygdala in different frequency bands

In the conventional frequency band (0.01–0.08 Hz), patients with ASD showed lower FC values between the left amygdala and left fusiform gyrus (FG). In the slow-4 frequency band (0.027–0.073 Hz), patients with ASD showed higher FC values between the left amygdala and left middle occipital gyrus (MOG). In the slow-5 frequency band (0.01–0.027 Hz), patients with ASD displayed lower FC values

TABLE 1 Demographic information of patients with ASD and TCs

| Site_ID | Participants | | Sex (M/F) | | | Age(years) | | |
	ASD	TCs	ASD M/F	TCs M/F	p-value	Mean (SD) ASD	TCs	p-value
001_BNI	19	18	19/0	18/0	—	37.84 (15.10)	38.39 (15.13)	.913
002_Caltech	3	3	3/0	3/0	—	20.77 (0.51)	20.87 (3.44)	.963
005_EMC	6	4	5/1	3/1	0.747	8.14 (0.93)	8.05 (0.96)	.878
006_ETH	4	4	4/0	4/0	—	20.94 (5.20)	21.35 (4.67)	.909
007_GU	9	9	9/0	9/0	—	11.64 (1.42)	11.45 (1.46)	.783
008_IP	10	10	6/4	5/5	0.653	22.99 (8.32)	20.74 (7.99)	.544
009_IU	8	8	7/1	7/1	1	21.88 (6.42)	23.13 (4.67)	.663
010_KKI1	2	2	2/0	2/0	—	9.41 (1.08)	9.91 (0.25)	.593
011_KKI2	6	18	5/1	13/5	0.586	10.18 (1.57)	10.17 (1.27)	.992
013_Leuven	16	15	14/2	12/3	0.570	17.64 (4.79)	17.99 (4.66)	.839
014_MaxMun1	6	6	5/1	5/1	1	29.83 (7.63)	30.50 (8.96)	.892
017_NYU1	45	56	38/7	49/7	0.659	15.75 (7.99)	15.72 (6.56)	.987
019_OHSU1	11	5	11/0	5/0	—	11.09 (1.91)	10.80 (0.67)	.670
020_OHSU2	22	22	16/6	16/6	1	10.86 (2.17)	11.00 (1.95)	.828
021_Olin1	3	3	3/0	3/0	—	17.00 (2.65)	17.00 (3.61)	.999
022_Olin2	5	5	4/1	4/1	1	21.00 (1.87)	21.20 (1.92)	.872
023_Pitt	11	8	9/2	6/2	0.719	18.68 (5.80)	18.80 (5.41)	.964
024_SBL	7	7	7/0	7/0	—	36.71 (7.54)	34.71 (5.38)	.578
025_SDSU	24	18	19/5	15/3	0.734	13.20 (3.04)	13.65 (1.44)	.527
026_Stanford1	4	4	2/2	2/2	1	9.55 (2.29)	9.60 (1.29)	.975
027_Stanford2	6	5	5/1	4/1	0.887	10.73 (1.85)	10.81 (1.69)	.943
028_Trinity1	10	15	10/0	15/0	—	17.24 (2.90)	17.29 (2.61)	.971
029_Trinity2	5	4	5/0	4/0	—	13.35 (3.77)	13.69 (1.28)	.870
030_UMIA	4	2	4/0	2/0	—	11.30 (2.22)	10.70 (0.85)	.742
031_UCD	4	5	3/1	4/1	0.858	15.54 (1.88)	15.52 (1.59)	.983
032_UCLA	25	24	21/4	20/4	0.950	12.44 (2.70)	12.42 (1.76)	.969
033_UM	17	18	12/5	13/5	0.915	14.07 (2.77)	14.06 (4.31)	.990
034_USM	14	16	14/0	16/0	—	22.34 (6.90)	22.28 (7.38)	.983

Note: There were no significant group differences for age and sex at each site (*p*-values > .05). There were no *p*-values for sex in 001_BNI, 002_Caltech, 006_ETH, 007_GU, 010_KKI1, 019_OHSU1, 021_Olin1, 024_SBL, 028_Trinity1, 029_Trinity2, 030_UMIA, and 034_USM due to the lack of female participants. The 003 and 004 sites were excluded due to poor normalization, whereas sites 012 and 018 were excluded due to the lack of TCs.
Abbreviations: ASD, autism spectrum disorder; F, female; M, male; TC, typical control.

between the left amygdala and left FG, as did the left amygdala and bilateral inferior temporal gyrus (ITG; Table 2 and Figure. 1).

3.2.2 | Altered FC results of the right amygdala in different frequency bands

When compared with TCs, patients with ASD showed lower FC values between the right amygdala and the orbital part of the left middle frontal gyrus (MFG) in the conventional frequency band (0.01–0.08 Hz). In the slow-4 frequency band (0.027–0.073 Hz), patients with ASD displayed higher FC values between the right

amygdala and right middle temporal gyrus (MTG). In the slow-5 frequency band (0.01–0.027 Hz), patients with ASD showed lower FC values between the right amygdala and the right SMG (Table 3 and Figure. 2).

3.3 | Classification accuracy in multifrequency bands

By taking the bilateral amygdala-based FC matrices as input, deep learning was used to distinguish patients with ASD from TCs using GANs and DNN models. As shown in Table 4, the frequency band of

TABLE 2 Altered functional connectivity results in the left amygdala in three frequency bands

Brain regions (AAL)	Number of voxels	MNI coordinate			Peak z-value	Effect size
		x	y	z		
Conventional frequency band (0.01–0.08 Hz)						
Fusiform_L	23	−40	−12	−44	−2.8739	−0.2419
Slow-4 frequency band (0.027–0.073 Hz)						
Occipital_Mid_L	25	−42	−84	0	3.9230	0.3258
Slow-5 frequency band (0.01–0.027 Hz)						
Fusiform_L	30	−36	−12	−42	−3.1048	−0.3024
Temporal_Inf_R	15	44	−10	−42	−3.2404	−0.2676
Temporal_Inf_L	10	−54	−18	−40	−3.0092	−0.2492

Note: z < 0 indicates that the FC value of the ASD group was lower than that of the TC group (*p* < .0001). Abbreviations: Fusiform_L, left fusiform gyrus; AAL, anatomical automatic labeling; ASD, autism spectrum disorder; FC, functional connectivity; L, left; MNI, Montreal Neurological Institute; Occipital_Mid_L, left middle occipital gyrus; R, right; TCs, typical control; Temporal_Inf_L, left inferior temporal gyrus; Temporal_Inf_R, right inferior temporal gyrus.
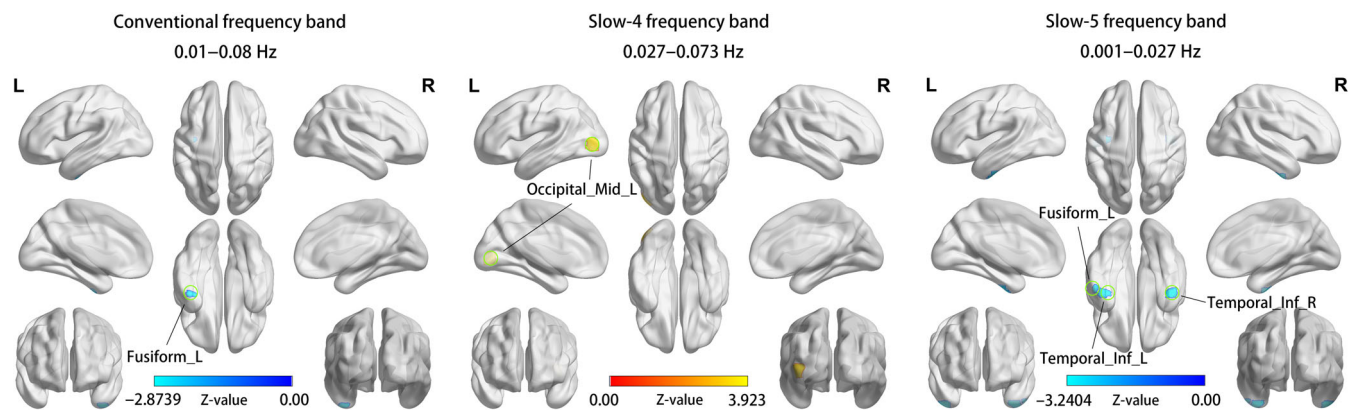
FIGURE 1 Altered functional connectivity (FC) of the left amygdala in three frequency bands. Altered FC results of the left amygdala in the conventional, slow-4, and slow-5 frequency bands in patients with autism spectrum disorder (ASD) compared with typical controls. The warm color represents the significantly increased FC value of patients with ASD, whereas the cold color represents the significantly decreased FC values of patients with ASD. The color bar represents z-value (*p* < .0001)

TABLE 3 Altered functional connectivity results in the right amygdala in three frequency bands

Brain regions (AAL)	Number of voxels	MNI coordinate			Peak z-value	Effect size
		x	y	z		
Conventional frequency band (0.01–0.08 Hz)						
Frontal_Mid_Orb_L	12	−30	40	−8	−2.5954	−0.2147
Slow-4 frequency band (0.027–0.073 Hz)						
Temporal_Mid_R	24	52	−2	−28	3.4887	0.2877
Slow-5 frequency band (0.01–0.027 Hz)						
SupraMarginal_R	10	62	−26	46	−2.8606	−0.2365

Note: z < 0 indicates that the FC value of the ASD group was lower than that of the TC group (*p* < .0001). Abbreviations: Frontal_Mid_Orb_L, orbital part of the left middle frontal gyrus; AAL, anatomical automatic labeling; ASD, autism spectrum disorder; FC, functional connectivity; L, left; MNI, Montreal Neurological Institute; R, right; SupraMarginal_R, right supramarginal gyrus; TCs, typical controls; Temporal_Mid_R, right middle temporal gyrus.

slow-5 (0.01–0.027 Hz) showed a higher area under the receiver operating characteristic curve (AUC) value of 0.811 than 0.639 in the slow-4 band (0.027–0.073 Hz) and 0.804 in the conventional band (0.01–0.08 Hz).

Moreover, compared with deep learning, which involves GANs, the results of deep learning without adopting GANs for feature generation showed a relatively poor classification effect. Detailed results are available in Figure S1 and Table S2.
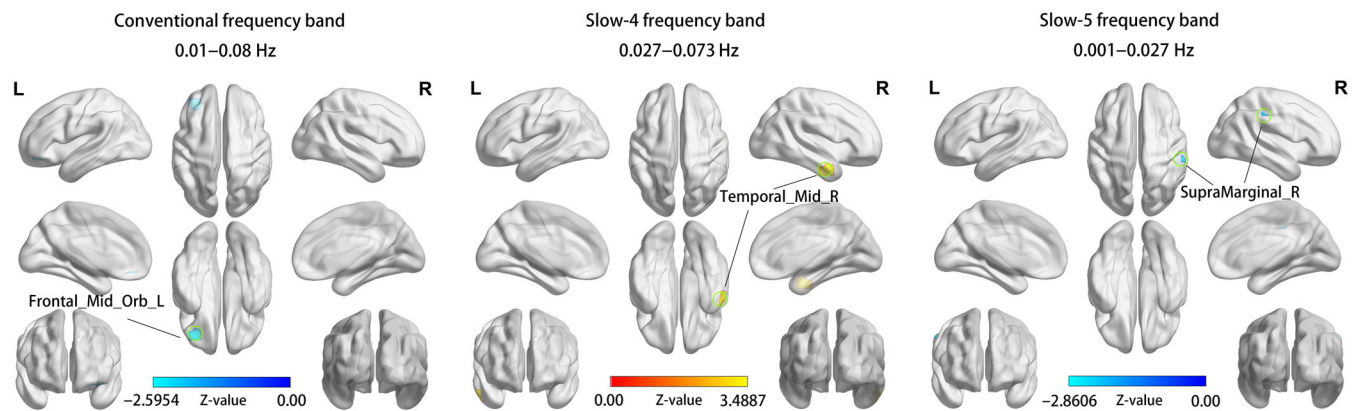
FIGURE 2 Altered functional connectivity (FC) results of the right amygdala in three frequency bands. Altered FC results of the right amygdala in the conventional, slow-4, and slow-5 frequency bands in patients with ASD compared with typical controls. The significantly increased FC values of patients with ASD are indicated in warm colors, whereas the decreased values are indicated in blue. The color bar represents the z-value with $p < .0001$

TABLE 4 The results of classification in three frequency bands

Frequency bands (Hz)	AUC Mean (±SD)	Accuracy Mean (±SD)	Precision Mean (±SD)	Recall Mean (±SD)
Conventional frequency band	0.804 (±0.0183)	73.39 (±2.83)	73.55 (±2.85)	73.06 (±2.94)
Slow-4 frequency band	0.639 (±0.0204)	60.03 (±2.38)	59.89 (±2.34)	60.70 (±2.57)
Slow-5 frequency band	0.811 (±0.0242)	74.73 (±2.78)	74.58 (±2.84)	75.05 (±2.77)

Note: The mean and SD values of the accuracy, precision, and recall metrics were reported as percentages (%), whereas the AUC was reported as decimals. Conventional frequency band: 0.01–0.08 Hz; Slow-4 frequency band: 0.027–0.073 Hz; Slow-5 frequency band: 0.01–0.027 Hz.
Abbreviations: AUC, area under the receiver operating characteristic curve; SD, standard deviation.

4 | DISCUSSION

In this study, we first adopted image-based meta-analyses to investigate altered FC of the bilateral amygdala in patients with ASD in three frequency bands, based on data collected from 28 sites in the ABIDE dataset. We then adopted a deep learning approach by combining GANs and DNN models to explore the classification ability of deep learning in different frequency bands. There are three main results: (1) The meta-analysis results revealed that in the conventional frequency band, patients with ASD showed lower FC values between the left amygdala and the left FG and between the right amygdala and the orbital part of the MFG; (2) The altered FC of the left amygdala showed frequency band specificity; (3) The deep learning results showed that, compared with the conventional and slow-4 frequency bands, the slow-5 frequency band showed the highest classification ability. These results revealed that the altered FC of the left amygdala was frequency specific, which may provide a deeper understanding of the pathological mechanism of ASD.

In this study, patients with ASD showed lower FC values between the left amygdala and left FG and between the right amygdala and the orbital part of the MFG. The FG and amygdala are part of the facial perception network and play critical roles in face processing (Dziobek et al., 2010). Previous studies have found that patients with ASD show activation in the amygdala and FG when presented with faces (Hadjikhani et al., 2004; Kuno-Fujita et al., 2020). Researchers have

found that the neural activity of the FG is regulated by the amygdala (Sato et al., 2019), and impaired connectivity between the FG and amygdala in patients with ASD has greatly impacted emotional face recognition (Schultz, 2005). Moreover, previous studies have indicated that, in addition to significant facial perception regions, facial perception has a connection with other cortical areas that belong to executive functions, such as attention control. The MFG, which is located in the middle part of the frontal cortex, plays an important role in attention reorientation in ASD (Japee et al., 2015). During the processing of facial recognition tasks, patients with ASD focus mainly on the mouth and pay very little attention to the eye region (Guillon et al., 2014). A previous rs-fMRI study found that patients with ASD showed lower FC values between the left amygdala and the frontal cortex (Christian et al., 2022), which was consistent with the findings of this study. Therefore, combining the previous findings and the present research, we assumed that the lower FC between the amygdala and the FG and MFG might provide novel insights into facial perception dysfunction in ASD.

In addition, compared with TCs, patients with ASD also showed a lower FC between the left amygdala and bilateral ITG and between the right amygdala and right SMG, and a higher FC between the right amygdala and right MTG. Situated in the temporal cortex, the ITG and MTG are associated with social and emotional information processing, including audiovisual sensory processing and multimodal emotional integration (Liu et al., 2021; Wright et al., 2003). Previous rs-FC

studies have shown that weaker connectivity between the amygdala and temporal lobe is correlated with increased autism severity (Shen et al., 2016), which could partly explain the results of this study. Located in the Wernicke area, the SMG is involved in auditory processing and plays a role in social communication (Wada et al., 2021; Wilson et al., 2022). Reduced FC of the SMG indicates deficient sensory integration in ASD (Wilson et al., 2022). Therefore, combining the role of the amygdala in emotional processing, we inferred that altered FC of the amygdala with the temporal regions and SMG might indicate an underlying deficient processing of social–emotional information in ASD.

Among the subfrequency bands, the FC of the left amygdala showed frequency band specificity. Regarding the left amygdala, patients with ASD exhibited lower FC in the left FG in the slow-5 and conventional frequency bands, higher FC in the left MOG in the slow-4 band, and lower FC in the bilateral ITG in the slow-5 band. The FC of the left amygdala and left FG were more sensitive to the slow-5 and conventional frequency bands. This result is consistent with previous studies showing frequency-dependent pathological mechanisms of patients with ASD (Chen et al., 2016; Duan et al., 2017). An rs-fMRI study of ASD investigating FC within and between large-scale cortical networks in multiple frequency bands found that weaker connectivity within and between specific networks in the slow-5 band was related to poorer social interaction and communication skills (Duan et al., 2017). Frequency band specificity has also been observed in other neuropsychiatric diseases. Yang, Yan, et al. (2020) observed a more varied fractional amplitude of low-frequency fluctuation (fALFF) values in the slow-5 band than in the slow-4 band in AD. Ren et al. (2022) explored the effect of transcranial direct current stimulation (tDCS) by assessing frequency-dependent alterations of fALFF and FC and found that the effect of tDCS on fALFF was significantly greater in the slow-5 band than in the slow-4 band. Evidence supported this study that the slow-5 frequency band can sensitively detect abnormal FC of the amygdala in patients with ASD and provides novel findings for the pathological mechanisms of ASD.

In this study, a deep learning approach that combines GANs and DNN methods was used to explore the diagnostic potential of different frequency bands in ASD. The deep learning results showed a frequency-dependent classification effect, indicating a better classification effect for the slow-5 band (AUC = 0.8110, accuracy = 0.7473) than for the conventional frequency band (AUC = 0.8040, accuracy = 0.7339) and slow-4 band (AUC = 0.6390, accuracy = 0.6063). This result was consistent with the findings of rs-FC in this study, suggesting the sensitivity of slow-5 and its importance in revealing the pathological mechanism of ASD. Furthermore, previous studies have shown that fMRI signals in subfrequency bands have a good classification effect in diagnosing patients with AD (Zhang et al., 2017), PD (Tian et al., 2020), and ASD (Chen et al., 2016). Therefore, we inferred that fMRI signals in the slow-5 frequency band might provide valuable information for the clinical diagnosis of ASD.

Despite these findings, this study has some limitations. In this study, although we obtained public data from the ABIDE database, the number of included participants was still not very large due to strict head motion exclusion standards. In future studies, we will consider including more participants from other autism databases and validating the results of this study. In addition, the data used in this study were obtained from the ABIDE public database, in which some sites or participant scales were not provided. Therefore, it is difficult to analyze the correlation between the FC values of regions that show group differences and scale scores, which leads to the failure to reveal the frequency specificity of the relationship between abnormal connectivity and the severity of autism symptoms.

5 | CONCLUSION

The altered FC in the left amygdala showed frequency specificity, which was sensitive to the slow-5 band. The deep learning results also showed frequency-specific classification ability. Specifically, the classification effect of the slow-5 band was better than that of the slow-4 and conventional bands. These findings could provide more insightful information on the pathological mechanism of ASD and are expected to provide insightful information for the treatment and diagnosis of ASD in future clinical practice.

AUTHOR CONTRIBUTIONS
Xize Jia, Yanyan Gao, Huibin Ma, and Yikang Cao conceived and designed this study. Yikang Cao executed the data analysis. Yikang Cao and Yanyan Gao wrote the first manuscript. Yanyan Gao, Mengting Li, Linlin Zhan, Lina Huang, and Zhou Xie helped coordinate the study and revised the manuscript. All authors have made significant scientific contributions to this article and reviewed the article.

CONFLICT OF INTEREST
The authors declared that this research has no financial conflicts of interest.

DATA AVAILABILITY STATEMENT
The fMRI data used in this study were obtained from the Autism Brain Imaging Data Exchange (http://fcon_1000.projects.nitrc.org/indi/abide/) public database.

ORCID
Xize Jia https://orcid.org/0000-0003-4698-8723

REFERENCES
Ambrosi, E., Arciniegas, D. B., Madan, A., Curtis, K. N., Patriquin, M. A., Jorge, R. E., Spalletta, G., Fowler, J. C., Frueh, B. C., & Salas, R. (2017). Insula and amygdala resting-state functional connectivity differentiate bipolar from unipolar depression. *Acta Psychiatrica Scandinavica*, *136*(1), 129–139.
Baron-Cohen, S. (2000). The amygdala theory of autism. *Neuroscience & Biobehavioral Reviews*, *24*(3), 355–364.

Bi, X.-A., Hu, X., Xie, Y., & Wu, H. (2021). A novel CERNNE approach for predicting Parkinson's disease-associated genes and brain regions based on multimodal imaging genetics data. *Medical Image Analysis*, 67, 101830.

Bi, X.-A., Zhou, W., Luo, S., Mao, Y., Hu, X., Zeng, B., & Xu, L. (2022). Feature aggregation graph convolutional network based on imaging genetic data for diagnosis and pathogeny identification of Alzheimer's disease. *Briefings in Bioinformatics*, 23(3), bbac137.

Biswal, B. B., Kylen, J. V., & Hyde, J. S. (2015). Simultaneous assessment of flow and BOLD signals in resting-state functional connectivity maps. *NMR in Biomedicine*, 10(4–5), 165–170. https://doi.org/10.1002/(SICI)1099-1492(199706/08)10:4/5<165::AID-NBM454>3.0.CO

Buzsaki, G., & Draguhn, A. (2004). Neuronal oscillations in cortical networks. *Science*, 304(5679), 1926–1929.

Chen, H., Duan, X., Liu, F., Lu, F., Ma, X., Zhang, Y., Uddin, L. Q., & Chen, H. (2016). Multivariate classification of autism spectrum disorder using frequency-specific resting-state functional connectivity—A multi-center study. *Progress in Neuro-Psychopharmacology and Biological Psychiatry*, 64, 1–9.

Chiarotti, F., & Venerosi, A. (2020). Epidemiology of autism spectrum disorders: A review of worldwide prevalence estimates since 2014. *Brain Sciences*, 10(5), 274. https://doi.org/10.3390/brainsci10050274

Christian, I. R., Liuzzi, M. T., Yu, Q., Kryza-Lacombe, M., Monk, C. S., Jarcho, J., & Wiggins, J. L. (2022). Context-dependent amygdala-prefrontal connectivity in youths with autism spectrum disorder. *Research in Autism Spectrum Disorders*, 91, 101913.

Di Martino, A., O'connor, D., Chen, B., Alaerts, K., Anderson, J. S., Assaf, M., Balsters, J. H., Baxter, L., Beggiato, A., Bernaerts, S., Blanken, L. M., Bookheimer, S. Y., Braden, B. B., Byrge, L., Castellanos, F. X., Dapretto, M., Delorme, R., Fair, D. A., Fishman, I., ... Bernaerts, S. (2017). Enhancing studies of the connectome in autism using the autism brain imaging data exchange II. *Scientific Data*, 4(1), 1–15. https://doi.org/10.1038/sdata.2017.10

Di Martino, A., Yan, C. G., Li, Q., Denio, E., Castellanos, F. X., Alaerts, K., Anderson, J. S., Assaf, M., Bookheimer, S. Y., Dapretto, M., Deen, B., Delmonte, S., Dinstein, I., Ertl-Wagner, B., Fair, D. A., Gallagher, L., Kennedy, D. P., Keown, C. L., Keysers, C., ... Milham, M. P. (2014). The autism brain imaging data exchange: Towards a large-scale evaluation of the intrinsic brain architecture in autism. *Molecular Psychiatry*, 19(6), 659–667. https://doi.org/10.1038/mp.2013.78

Duan, X., Chen, H., He, C., Long, Z., Guo, X., Zhou, Y., Uddin, L. Q., & Chen, H. (2017). Resting-state functional under-connectivity within and between large-scale cortical networks across three low-frequency bands in adolescents with autism. *Progress in Neuro-Psychopharmacology and Biological Psychiatry*, 79, 434–441.

Dziobek, I., Bahnemann, M., Convit, A., & Heekeren, H. R. (2010). The role of the fusiform-amygdala system in the pathophysiology of autism. *Archives of General Psychiatry*, 67(4), 397–405.

Epalle, T. M., Song, Y., Liu, Z., & Lu, H. (2021). Multi-atlas classification of autism spectrum disorder with hinge loss trained deep architectures: ABIDE I results. *Applied Soft Computing*, 107, 107375.

Fombonne, E. (2018). Editorial: The rising prevalence of autism. *Journal of Child Psychology and Psychiatry*, 59(7), 717–720. https://doi.org/10.1111/jcpp.12941

Fox, M., & Raichle, M. E. (2007). Spontaneous fluctuations in brain activity observed with functional magnetic resonance imaging. *Nature Reviews Neuroscience*, 8(9), 700–711.

Friston, K. J., Williams, S., Howard, R., Frackowiak, R. S., & Turner, R. (1996). Movement-related effects in fMRI time-series. *Magnetic Resonance in Medicine*, 35(3), 346–355. https://doi.org/10.1002/mrm.1910350312

Geschwind, D. H., & Levitt, P. (2007). Autism spectrum disorders: Developmental disconnection syndromes. *Current Opinion in Neurobiology*, 17(1), 103–111.

Goodfellow, I., Pouget-Abadie, J., Mirza, M., Xu, B., Warde-Farley, D., Ozair, S., Courville, A., & Bengio, Y. (2020). Generative adversarial networks. *Communications of the ACM*, 63(11), 139–144. https://doi.org/10.1145/3422622

Guillon, Q., Hadjikhani, N., Baduel, S., & Rogé, B. (2014). Visual social attention in autism spectrum disorder: Insights from eye tracking studies. *Neuroscience & Biobehavioral Reviews*, 42, 279–297.

Guo, X., Duan, X., Long, Z., Chen, H., Wang, Y., Zheng, J., ... Chen, H. (2016). Decreased amygdala functional connectivity in adolescents with autism: A resting-state fMRI study. *Psychiatry Research: Neuroimaging*, 257, 47–56.

Hadjikhani, N., Joseph, R. M., Snyder, J., Chabris, C. F., Clark, J., Steele, S., McGrath, L., Vangel, M., Aharon, I., Feczko, E., Harris, G. J., & Tager-Flusberg, H. (2004). Activation of the fusiform gyrus when individuals with autism spectrum disorder view faces. *NeuroImage*, 22(3), 1141–1150.

Huang, Z.-A., Zhu, Z., Yau, C. H., & Tan, K. C. (2020). Identifying autism spectrum disorder from resting-state fMRI using deep belief network. *IEEE Transactions on Neural Networks and Learning Systems*, 32(7), 2847–2861.

Japee, S., Holiday, K., Satyshur, M. D., Mukai, I., & Ungerleider, L. G. (2015). A role of right middle frontal gyrus in reorienting of attention: A case study. *Frontiers in Systems Neuroscience*, 9, 23.

Jia, X.-Z., Wang, J., Sun, H.-Y., Zhang, H., Liao, W., Wang, Z., Yan, C.-G., Song, X.-W., & Zang, Y.-F. (2019). RESTplus: An improved toolkit for resting-state functional magnetic resonance imaging data processing. *Scientific Bulletin*, 64, 953–954.

Jiang, W., Liu, S., Zhang, H., Sun, X., Wang, S.-H., Zhao, J., & Yan, J. (2022). CNNG: A convolutional neural networks with gated recurrent units for autism Spectrum disorder classification. *Frontiers in Aging Neuroscience*, 14, 948704.

Kuno-Fujita, A., Iwabuchi, T., Wakusawa, K., Ito, H., Suzuki, K., Shigetomi, A., Hirotaka, K., Tsujii, M., & Tsuchiya, K. J. (2020). Sensory processing patterns and fusiform activity during face processing in autism spectrum disorder. *Autism Research*, 13(5), 741–750.

LeCun, Y., Bengio, Y., & Hinton, G. (2015). Deep learning. *Nature*, 521(7553), 436–444.

Li, J., Cheng, L., Chen, S., Zhang, J., Liu, D., Liang, Z., & Li, H. (2022). Functional connectivity changes in multiple-frequency bands in acute basal ganglia ischemic stroke patients: A machine learning approach. *Neural Plasticity*, 2022, 1–10.

Li, L., He, C., Jian, T., Guo, X., Xiao, J., Li, Y., Chen, H., Kang, X., Chen, H., & Duan, X. (2021). Attenuated link between the medial prefrontal cortex and the amygdala in children with autism spectrum disorder: Evidence from effective connectivity within the "social brain". *Progress in Neuro-Psychopharmacology and Biological Psychiatry*, 111, 110147.

Li, S., Tang, Z., Jin, N., Yang, Q., Liu, G., Liu, T., Hu, J., Liu, S., Wang, P., Hao, J., Zhang, Z., Zhang, X., Li, J., Wang, X., Li, Z., Wang, Y., Yang, B., & Ma, L. (2022). Uncovering brain differences in preschoolers and young adolescents with autism spectrum disorder using deep learning. *International Journal of Neural Systems*, 32, 2250044.

Liu, P., Sutherland, M., & Pollick, F. E. (2021). Incongruence effects in cross-modal emotional processing in autistic traits: An fMRI study. *Neuropsychologia*, 161, 107997.

Lord, C., Elsabbagh, M., Baird, G., & Veenstra-Vanderweele, J. (2018). Autism spectrum disorder. *The Lancet*, 392(10146), 508–520.

Lozier, L. M., Vanmeter, J. W., & Marsh, A. A. (2014). Impairments in facial affect recognition associated with autism spectrum disorders: A meta-analysis. *Development and Psychopathology*, 26(4pt1), 933–945.

Minshew, N. J., & Keller, T. A. (2010). The nature of brain dysfunction in autism: Functional brain imaging studies. *Current Opinion in Neurology*, 23(2), 124–130.

Misra, V. (2014). The social brain network and autism. *Annals of Neurosciences*, 21(2), 69.

Odriozola, P., Dajani, D. R., Burrows, C. A., Gabard-Durnam, L. J., Goodman, E., Baez, A. C., Tottenham, N., Uddin, L. Q., & Gee, D. G. (2019). Atypical frontoamygdala functional connectivity in youth with autism. *Developmental Cognitive Neuroscience*, *37*, 100603.

Park, J. E., Eun, D., Kim, H. S., Lee, D. H., Jang, R. W., & Kim, N. (2021). Generative adversarial network for glioblastoma ensures morphologic variations and improves diagnostic model for isocitrate dehydrogenase mutant type. *Scientific Reports*, *11*(1), 1–11.

Penttonen, M., & Buzsáki, G. (2003). Natural logarithmic relationship between brain oscillators. *Thalamus & Related Systems*, *2*(2), 145–152.

Radua, J., Mataix-Cols, D., Phillips, M. L., El-Hage, W., Kronhaus, D. M., Cardoner, N., & Surguladze, S. (2012). A new meta-analytic method for neuroimaging studies that combines reported peak coordinates and statistical parametric maps. *European Psychiatry*, *27*(8), 605–611. https://doi.org/10.1016/j.eurpsy.2011.04.001

Radua, J., Rubia, K., Canales, E. J., Pomarol-Clotet, E., Fusar-Poli, P., & Mataix-Cols, D. (2014). Anisotropic kernels for coordinate-based meta-analyses of neuroimaging studies. *Frontiers in Psychiatry*, *5*, 13.

Ramzan, F., Khan, M. U. G., Rehmat, A., Iqbal, S., Saba, T., Rehman, A., & Mehmood, Z. (2020). A deep learning approach for automated diagnosis and multi-class classification of Alzheimer's disease stages using resting-state fMRI and residual neural networks. *Journal of Medical Systems*, *44*(2), 1–16.

Ren, P., Ma, M., Wu, D., & Ma, Y. (2022). Frontopolar tDCS induces frequency-dependent changes of spontaneous low-frequency fluctuations: A resting-state fMRI study. *Cerebral Cortex*, *32*(16), 3542–3552.

Salimi-Khorshidi, G., Smith, S. M., Keltner, J. R., Wager, T. D., & Nichols, T. E. (2009). Meta-analysis of neuroimaging data: A comparison of image-based and coordinate-based pooling of studies. *NeuroImage*, *45*(3), 810–823. https://doi.org/10.1016/j.neuroimage.2008.12.039

Sato, W., Kochiyama, T., Uono, S., Yoshimura, S., Kubota, Y., Sawada, R., Sakihama, M., & Toichi, M. (2017). Reduced gray matter volume in the social brain network in adults with autism spectrum disorder. *Frontiers in Human Neuroscience*, *11*, 395.

Sato, W., Kochiyama, T., Uono, S., Yoshimura, S., Kubota, Y., Sawada, R., Sakihama, M., & Toichi, M. (2019). Atypical amygdala–neocortex interaction during dynamic facial expression processing in autism spectrum disorder. *Frontiers in Human Neuroscience*, *13*, 351.

Sato, W., Toichi, M., Uono, S., & Kochiyama, T. (2012). Impaired social brain network for processing dynamic facial expressions in autism spectrum disorders. *BMC Neuroscience*, *13*(1), 1–17.

Sato, W., & Uono, S. (2019). The atypical social brain network in autism: Advances in structural and functional MRI studies. *Current Opinion in Neurology*, *32*(4), 617–621. https://doi.org/10.1097/wco.0000000000000713

Schultz, R. T. (2005). Developmental deficits in social perception in autism: The role of the amygdala and fusiform face area. *International Journal of Developmental Neuroscience*, *23*(2–3), 125–141.

Shahamiri, S. R., Thabtah, F., & Abdelhamid, N. (2022). A new classification system for autism based on machine learning of artificial intelligence. *Technology and Health Care*, *30*(3), 1–18.

Shen, M. D., Li, D. D., Keown, C. L., Lee, A., Johnson, R. T., Angkustsiri, K., Rogers, S. J., Müller, R. A., Amaral, D. G., & Nordahl, C. W. (2016). Functional connectivity of the amygdala is disrupted in preschool-aged children with autism Spectrum disorder. *Journal of the American Academy of Child and Adolescent Psychiatry*, *55*(9), 817–824. https://doi.org/10.1016/j.jaac.2016.05.020

Shou, X.-J., Xu, X.-J., Zeng, X.-Z., Liu, Y., Yuan, H.-S., Xing, Y., Jia, M. X., Wei, Q. Y., Han, S. P., Zhang, R., & Han, J. S. (2017). A volumetric and functional connectivity MRI study of brain arginine-vasopressin pathways in autistic children. *Neuroscience Bulletin*, *33*(2), 130–142.

Sinha, S., Thomopoulos, S. I., Lam, P., Muir, A., & Thompson, P. M. (2021). Alzheimer's disease classification accuracy is improved by MRI harmonization based on attention-guided generative adversarial networks.

Paper presented at the 17th international symposium on medical information processing and analysis.

Skuse, D., Morris, J., & Lawrence, K. (2003). The amygdala and development of the social brain. *Annals of the New York Academy of Sciences*, *1008*(1), 91–101.

Supekar, K., de Los Angeles, C., Ryali, S., Cao, K., Ma, T., & Menon, V. (2022). Deep learning identifies robust gender differences in functional brain organization and their dissociable links to clinical symptoms in autism. *The British Journal of Psychiatry*, *220*(4), 202–209.

Tian, Z.-Y., Qian, L., Fang, L., Peng, X.-H., Zhu, X.-H., Wu, M., Wang, W. Z., Zhang, W. H., Zhu, B. Q., Wan, M., Hu, X., & Shao, J. (2020). Frequency-specific changes of resting brain activity in Parkinson's disease: A machine learning approach. *Neuroscience*, *436*, 170–183.

Tomasi, D., & Volkow, N. D. (2019). Reduced local and increased Long-range functional connectivity of the thalamus in autism Spectrum disorder. *Cerebral Cortex*, *29*(2), 573–585. https://doi.org/10.1093/cercor/bhx340

Tzourio-Mazoyer, N., Landeau, B., Papathanassiou, D., Crivello, F., Etard, O., Delcroix, N., Mazoyer, B., & Joliot, M. (2002). Automated anatomical labeling of activations in SPM using a macroscopic anatomical parcellation of the MNI MRI single-subject brain. *NeuroImage*, *15*(1), 273–289.

Wada, S., Honma, M., Masaoka, Y., Yoshida, M., Koiwa, N., Sugiyama, H., Iizuka, N., Kubota, S., Kokudai, Y., Yoshikawa, A., Kamijo, S., Kamimura, S., Ida, M., Ono, K., Onda, H., & Izumizaki, M. (2021). Volume of the right supramarginal gyrus is associated with a maintenance of emotion recognition ability. *PLoS One*, *16*(7), e0254623.

Wang, G., Lyu, H., Wu, R., Ou, J., Zhu, F., Liu, Y., Zhao, J., & Guo, W. (2020). Resting-state functional hypoconnectivity of amygdala in clinical high risk state and first episode schizophrenia. *Brain Imaging and Behavior*, *14*(5), 1840–1849.

Wang, L., Kong, Q., Li, K., Su, Y., Zeng, Y., Zhang, Q., Dai, W., Xia, M., Wang, G., Jin, Z., Yu, X., & Si, T. (2016). Frequency-dependent changes in amplitude of low-frequency oscillations in depression: A resting-state fMRI study. *Neuroscience Letters*, *614*, 105–111.

Wang, P., Li, R., Yu, J., Huang, Z., & Li, J. (2016). Frequency-dependent brain regional homogeneity alterations in patients with mild cognitive impairment during working memory state relative to resting state. *Frontiers in Aging Neuroscience*, *8*, 60.

Wang, Q., Li, H. Y., Li, Y. D., Lv, Y. T., Ma, H. B., Xiang, A. F., Jia, X. Z., & Liu, D. Q. (2021). Resting-state abnormalities in functional connectivity of the default mode network in autism spectrum disorder: A meta-analysis. *Brain Imaging and Behavior*, *15*(5), 2583–2592. https://doi.org/10.1007/s11682-021-00460-5

Wang, Q., Wang, C., Deng, Q., Zhan, L., Tang, Y., Li, H., Antwi, C. O., Xiang, A., Lv, Y., Jia, X., & Ren, J. (2022). Alterations of regional spontaneous brain activities in anxiety disorders: A meta-analysis. *Journal of Affective Disorders*, *296*, 233–240.

Wang, X., Chen, L., Liu, P., Polk, R. J., & Feng, T. (2020). Orientation to and processing of social stimuli under normal and competitive conditions in children with autism spectrum disorder. *Research in Autism Spectrum Disorders*, *78*, 101614.

Wee, C. Y., Yap, P. T., & Shen, D. (2016). Diagnosis of autism spectrum disorders using temporally distinct resting-state functional connectivity networks. *CNS Neuroscience & Therapeutics*, *22*(3), 212–219.

Wilson, K. C., Kornisch, M., & Ikuta, T. (2022). Disrupted functional connectivity of the primary auditory cortex in autism. *Psychiatry Research: Neuroimaging*, *324*, 111490.

Wright, T. M., Pelphrey, K. A., Allison, T., McKeown, M. J., & McCarthy, G. (2003). Polysensory interactions along lateral temporal regions evoked by audiovisual speech. *Cerebral Cortex*, *13*(10), 1034–1043.

Yang, L., Yan, Y., Li, Y., Hu, X., Lu, J., Chan, P., Yan, T., & Han, Y. (2020). Frequency-dependent changes in fractional amplitude of low-frequency oscillations in Alzheimer's disease: A resting-state fMRI study. *Brain Imaging and Behavior*, *14*(6), 2187–2201.

Yang, X., Schrader, P. T., & Zhang, N. (2020). A deep neural network study of the ABIDE repository on autism spectrum classification. *International Journal of Advanced Computer Science and Applications*, *11*(4), 1–6.

Yao, S., Becker, B., & Kendrick, K. M. (2021). Reduced inter-hemispheric resting state functional connectivity and its association with social deficits in autism. *Frontiers in Psychiatry*, *12*, 629870. https://doi.org/10.3389/fpsyt.2021.629870

Yi, X., Walia, E., & Babyn, P. (2019). Generative adversarial network in medical imaging: A review. *Medical Image Analysis*, *58*, 101552.

Zhang, Z., Liao, M., Yao, Z., Hu, B., Xie, Y., Zheng, W., Hu, T., Zhao, Y., Yang, F., Zhang, Y., Su, L., Li, L., Gutknecht, J., & Majoe, D. (2017). Frequency-specific functional connectivity density as an effective biomarker for adolescent generalized anxiety disorder. *Frontiers in Human Neuroscience*, *11*, 549.

Zhao, F., Chen, Z., Rekik, I., Lee, S.-W., & Shen, D. (2020). Diagnosis of autism spectrum disorder using central-moment features from low- and high-order dynamic resting-state functional connectivity networks. *Frontiers in Neuroscience*, *14*, 258.

Zhao, J., Huang, J., Zhi, D., Yan, W., & Sui, J. (2020). Functional network connectivity (FNC)-based generative adversarial network (GAN) and its applications in classification of mental disorders. *Journal of Neuroscience Methods*, *341*, 108756.

Zhao, L., Xue, S.-W., Sun, Y.-K., Lan, Z., Zhang, Z., Xue, Y., Wang, X., & Jin, Y. (2021). Altered dynamic functional connectivity of insular subregions could predict symptom severity of male patients with autism spectrum disorder. *Journal of Affective Disorders*, *299*, 504–512. https://doi.org/10.1016/j.jad.2021.12.093

Zhou, X., Qiu, S., Joshi, P. S., Xue, C., Killiany, R. J., Mian, A. Z., Chin, S. P., Au, R., & Kolachalama, V. B. (2021). Enhancing magnetic resonance imaging-driven Alzheimer's disease classification performance using generative adversarial learning. *Alzheimer's Research & Therapy*, *13*(1), 1–11.

Zuo, X.-N., Di Martino, A., Kelly, C., Shehzad, Z. E., Gee, D. G., Klein, D. F., Castellanos, F. X., Biswal, B. B., & Milham, M. P. (2010). The oscillating brain: Complex and reliable. *NeuroImage*, *49*(2), 1432–1445.

SUPPORTING INFORMATION

Additional supporting information can be found online in the Supporting Information section at the end of this article.